Sustainable Biogenic Synthesis of Silver Nanoparticles (AgNPs) using *Aegle marmelos* and Evaluation of their Photocatalytic, Antimicrobial and Cytotoxicity Properties

Abhinash Marukurti[1*], Alavala Matta Reddy[1], V Durga Praveena[2], G Tejaswini[2], M Padmaja[2], L Rajeswari[2], D Sailaja[3], P Vijaya Nirmala[1], N Baby Nirmala[2], J Shashi Sri[2]

[1]School of Life and Health Sciences, Adikavi Nannaya University, Rajamahendravaram
[2]Department of Chemistry, Government College (A) Rajamahendravaram
[3]Department of Zoology, Government College (A) Rajamahendravaram

Corresponding author:
abhinashmarukurti@gmail.com

Abstract:

Nanotechnology has revolutionized materials research, leveraging nanoscale entities (1–100 nm) with extensive applications across diverse fields. This study explores the synthesis of silver nanoparticles (AgNPs) using aqueous leaf extract of *Aegle marmelos* (AMLAE) prepared via the decoction method. The Ag^+ ions were reduced to Ag^0 using AMLAE and without using any chemical for reduction and precipitation. The formation of AM-AgNPs was confirmed through UV-Vis spectroscopy, which exhibited a localized surface plasmon resonance (LSPR) band at 450 nm. Fourier-transform infrared (FTIR) analysis revealed surface functionalization, including O-H, C=C, C=O, and Ag-O bonds. X-ray diffraction (XRD) confirmed a face-centered cubic structure with an average crystallite size of 14.07 nm, while high-resolution transmission electron microscopy (HRTEM) indicated spherical morphology and an average particle size of 16.07 nm. Dynamic light scattering (DLS) analysis showed a hydrodynamic size of 237.5 nm with a polydispersity index (PDI) of 0.243 and a zeta potential of -16.6 mV, indicating colloidal stability. The antimicrobial efficacy of AM-AgNPs was assessed against six pathogens, with minimum inhibitory concentrations (MIC) as low as 15.62 µg mL^{-1} for *Vibrio parahaemolyticus*. Photocatalytic degradation of methylene blue (50 ppm) demonstrated a 99.24% degradation efficiency under visible light within 60 minutes. Cytotoxicity studies on Vero cell lines yielded an IC50 value of 253.73 µg mL^{-1}, suggesting low toxicity levels. These findings represent the potential of green-synthesized AgNPs for biomedical and environmental applications, establishing AMLAE as an efficient and sustainable reducing agent.

Keywords: Nanotechnology, Silver Nanoparticles, *Aegle marmelos*, cytotoxicity.

R. K. Ramachandra et al. (eds.), *Proceedings of the International Conference on Bio-Based Environment for Sustainable Territory (IC-BEST 2024)*, Advances in Biological Sciences Research 44,
https://doi.org/10.2991/978-94-6463-648-2_15

1. Introduction

The renowned scientist Richard Feynman conceptualized nanotechnology in 1959 and this branch of science has initiated a novel epoch in materials research with extensive applications in physics, chemistry, biological sciences, electronics, medicine, catalysis, optics, and bioengineering [1]. Nanotechnology deals with the study of nanoscale entities (1-100 nm) and is listed in the European Commission's six "Key Enabling Technologies" acknowledged for its contribution to sustainable competitiveness and growth across diverse industrial applications [2]. The synthesis of nanoparticles (NPs) has been thoroughly investigated due to their dimensions (1–100 nm), high surface area, and distinctive physiochemical characteristics, which provide numerous potential applications [3]. The application of nanoparticles, referred to as 'Bhasma,' in therapeutic research at the nano-scale was initially documented over 5,000 years ago in Ayurveda [4]. The worldwide recognition of green nanotechnology is increasing, since it encompasses many methods that limits the use of toxic chemical compounds in synthesis of NPs and eco-friendly in nature [5]. Green synthesis of nanoparticles is chosen more often because of different qualities such as the low cost involved, minimal likelihood of mishaps, greater economical benefits, safe products, and suitability for pharmacy-based industries [6]. Among various nanoparticles, silver nanoparticles (AgNPs) are among the most significant and intriguing nanomaterials utilized in numerous biomedical applications. They have acquired prominence in recent years owing to their diverse applications, including antioxidant, antibacterial, anti-angiogenic, wound healing, anti-inflammatory, anticancer properties, cost-effectiveness, and environmentally friendly characteristics [7].

Bael (*Aegle marmelos* (L.) Corr.), commonly known as wood apple, belongs to the Rutaceae family is an Indian medicinal plant which has enormous traditional values against various diseases [8]. Bael is considered an economically important tree species as it possesses multiple benefits: it is used as an element for the medical preparations of herbs and is popular for making pudding, jams, and syrup [8]. The different parts of Bael contain bioactive components, including various phytoconstituents such as marceline, xanthotoxol, alkaloids, coumarin, coumarins, terpenoids, fatty acids, amino acids, marceline, xanthotoxol, angeline, and imperatorin, with various pharmaceutical applications such as antifertility, insecticidal, immunogenic, and antidiabetic activities. *A. marmelos* is widely used in Ayurvedic and folk medicines to cure peptic ulcers, tuberculosis, headache, hypertension, dysentery, and diabetes [9].

Several previous studies reported the synthesis of AgNPs using various parts of *A. marmelos* and different extraction methods. The AgNPs synthesized using leaves (Decoction method) [10], [11], [12], [13], fruit (agitation and maceration) [14], fruit (decoction) [15], and bark (decoction) [16] reported biological and photocatalytic properties. Despite of the advantages, these previous studies reported has several limitations. To explore more applications, the present study aims to synthesize AgNPs using leaves of *A. marmelos* and the reducing agent was prepared using decoction method. Thus, the objectives of the present study are (1) To synthesize the AgNPs using leaf extract of *A. marmelos* (2) To understand the synthesized properties of AM-AgNPs using various analytical techniques and (3) To study the photocatalytic, antimicrobial and healthy cell line cytotoxicity.

2. Materials and Methods:

2.1. Preparation of *Aegle marmelos* aqueous leaf extract (AMALE):

The fresh leaves of *Aegle marmelos* were collected from the Adikavi Nannaya University campus and shade dried for 7 days until complete evaporation of moisture. The pulverized powder of *Aegle marmelos leaves was* further subjected to preparation of aqueous extract using the decoction method [17]. This method involved suspending 5 g of pulverized powder in 100 mL of double-distilled water, followed by an incubation period of 20 min at 60°C in a water bath. After incubation, the solution was cooled down to room temperature and filtered using a Buchner funnel, muslin cloth, and Whatman filter paper No. 1, respectively, and the final solution was labelled as AMLAE.

2.2. Green synthesis of silver nanoparticles (AgNPs):

The green synthesis of AgNPs was carried out using the bio-reduction method [18], where AMLAE was used as the reducing agent and no other chemical reducing or precipitating agent was used in this study. Briefly, 10 mM of silver nitrate ($AgNO_3$) was dissolved in distilled water, and the solution was wrapped with aluminum foil to prevent light irradiation and kept on a magnetic stirrer with a hot plate at 70°C. The solution was allowed to achieve heat, and the reducing agent, AMLAE, was slowly released into the $AgNO_3$ solution. Phytochemicals or secondary metabolites present in the AMLAE contribute to the reduction of Ag^+ ions, and these molecules also serve as capping and stabilizing agents. After the addition of AMLAE, the reaction mixture was further irradiated with sunlight, which may enhance the formation and stabilization of AgNPs. After 3 hours, the obtained AM-AgNPs were collected by centrifugation and washed three times with 70% ethanol.

2.3. Analysis of optical and morphological properties of AM-AgNPs:

The localized surface plasmon resonance (LSPR) of AgNPs was observed at 200-800 nm wavelength using a UV-visible spectrophotometer. The surface functionalization of AMLAE and AM-AgNPs was analyzed using Fourier transform infrared spectroscopy (FTIR) from 500 to 4000 cm^{-1}. The phase analysis, diffractogram, and average crystallite size were carried out using X-ray diffraction (XRD) at a 2θ angle (10 to 90°). High-resolution transmission electron microscopy (HRTEM) observed the size distribution and selected area electron diffraction (SAED) pattern, while field emission scanning electron microscopy (FESEM-EDX) carried out the surface morphology and elemental distribution. The hydrodynamic size and zeta potential were evaluated using a Zeta sizer. The obtained raw data of all the analytical methods was further subjected to analysis using Origin Pro, Xpert Hiscore, and Image J software.

2.4. Antimicrobial activity of AM-AgNPs:

Broth microdilution (BMD) was used to assess the minimum inhibitory concentration (MIC) of AM-AgNPs on 6 significant pathogenic organisms, namely *Vibrio parahaemolyticus* (MTCC 451), *Staphylococcus aureus* (MTCC 87), *Streptococcus pyogenes* (MTCC 442), *Candida albicans* (MTCC 183), *Vibrio harveyi* (ATCC 14126), and *Aspergillus niger* (MTCC 282). Using the two-fold dilution method, we added 5% DMSO-dissolved AM-AgNPs to LB broth, containing a microbial inoculum of 10^5 CFU mL^{-1}. We also added 1% TTC solution to all the wells, maintaining both positive and negative controls. After a 24-hour incubation period, the wells containing concentrations of AM-AgNPs that did not develop a pink or red color are considered to have the MIC value.

2.5. Photocatalytic Degradation of AM-AgNPs:

The photocatalytic degradation of AM-AgNPs was carried out on 50 ppm of methylene blue (aqueous) concentration under irradiation of visible light (100 W) for 60 minutes with a time interval of every 10 min. 100 µg mL^{-1} of AM-AgNPs were added to the methylene blue solution, and a sample was taken every 10 min, and absorbance was measured at 664 nm.

2.6. Vero cell cytotoxicity:

Vero cell lines are healthy (non-cancerous) cell line model used for the study the cytotoxicity effect of natural and synthesized drug materials. In the present study, different concentrations of AM-AgNPs (0 to 200 µg mL^{-1}) were treated on Vero cell lines and the cell viability (%) was analysed at each concentration. In brief, the cells were revived from -20°C refrigerator into DMEM medium supplied with 10% fetal calf serum. The revived cells were incubated with sample of different concentration for 48 h at 37°C in a CO_2 incubator. After incubation, the cells were treated with MTT reagent and cell viability (%) was estimated by taking absorbance at 540 nm using ELISA plate reader [56]. The Vero cell line viability (%) was estimated using equation 1.

$$Cell\ viability\ (\%) = \frac{Absorbance\ of\ control\ well - Absorban\ \ of\ sample\ well}{Absorbance\ of\ control\ well} \times 100 \quad (1)$$

3. Result and Discussion:

To meet green chemistry principles, the synthesis of metallic nanoparticles using plants and microbial extracts has gained research interest since the last few decades. Plant phytochemicals serve as efficient reducing and stabilizing agents, and their extraction process depends upon reaction time, reaction temperature, solvent, etc [19]. The present study utilized AMLAE as a reducing agent for the synthesis of AgNPs because it is one of the prominent medicinal plants utilized in Ayurveda.

3.1. LSPR, Surface functional groups and Phase analysis of AM AgNPs:

The addition of AMALE to the 10 mM $AgNO_3$ ssolution results in the appearance of a low-intensity localized surface plasmon resonance (LSPR) band at 450 nm, which was observed using UV-Vis spectroscopy (Fig 1(a)). The appearance of low-intensity LSPR may be due to the over capping of phytochemicals from AMLAE on silver ions. Similar studies were reported the appearance of LSPR for AgNPs synthesized using fruit and leaves of *Aegle marmelos* between 400-470 nm [10], [14]. LSPR identification only confirms the formation of AgNPs, not the surface functionalization. The biomedical and environmental applications of green AgNPs are directly proportional to the surface functional groups (AMLAE phytochemicals in this study). Figs. 1(b) and (c) represent the FTIR analyses of AMLAE and AM-AgNPs. AMLAE shows two major vibrational signals at 3309 cm^{-1} (O-H stretching) and 1632 cm^{-1} (C=O stretching) and a minor vibrational signal at 2114 cm^{-1} (C≡C stretching), and the presence of these functional groups is correlated with phytochemicals polyphenols and flavonoids. The addition of AMLAE to the silver precursor results in the appearance of new vibrational stretching. AM-AgNPs consists of the following vibrational stretching peaks at 3232 cm^{-1} (O-H stretching), 1584 cm^{-1} (C=C stretching), 1351 and 1056 cm^{-1} (C-O stretching), and a vibrational signal between 826–610 cm^{-1} (Ag-O bond). These results confirmed the reduction of AgNPs by AMLAE, and the transitions of stretching vibrations may be due to the interaction of various phytochemicals with Ag ions.

The phase analysis and average crystallite size of AM-AgNPs were measured using XRD analysis (Fig. 1(d)). The diffraction peaks of AM AgNPs are found, and corresponding hkl values at 2θ angles of 38.20° (1 1 1), 44.40° (2 0 0), 66.60° (2 2 0), 77.59° (3 1 1), and 81.75° (2 2 2) correspond to face-centered cubic (fcc) silver. The diffraction data is correlated with the standard JCPDS card no. 01-087-0718 (silver), and the calculated average crystallite size using the Scherrer equation is 14.07 nm. The unassigned peaks of diffractogram represents the crystallization of phytochemicals on surface of AM-AgNPs.

3.2 Morphology, Size Distribution and Zeta Potential:

The surface morphology, topology, and elemental composition of AM-AgNPs were studied using FESEM-EDAX. Fig 2(a) represents the well-dispersed and spherical-shaped nanoparticles, and a strong signal of Ag at 3 keV was in EDAX confirmed the formation of AM-AgNPs (Fig 2(b)). The appearance of other elements such as C, O, Al, Cl, and K in EDAX in traces may be from AMLAE. The amorphous nature of AM-AgNPs was analyzed using selected area electron diffraction (SAED) patterns and correlated with diffraction angles of the XRD pattern (Fig. 2(d)). The HRTEM micrograph (Fig. 2(c)) shows homogeneously dispersed nanoparticles with a particle size distribution of 0-35 nm and an average particle diameter of 16.07 nm (Fig. 3(a)).

DLS analysis determines the hydrodynamic size and zeta potential of AM-AgNPs, which helps in understanding the colloidal stability and interparticle forces of interaction [20]. The average hydrodynamic size/eta size of AM-AgNPs was 237.5 d.nm, and a calculated polydispersity index (PDI) of 0.243 was obtained (Fig. 3(b)). The surface charge of -16.6 ± 4.95 was identified using zeta potential with a conductivity of 0.0363 (Fig. 3(c)). The average hydrodynamic size of nanoparticles is greater than the average crystallite size and average particle size diameter, and the similar was observed in the present study. The PDI value, which ranges from 0 to 1, indicates a homogeneous distribution of AM-AgNPs with minimal particle agglomeration. The negative zeta potential value represents the stability of nanoparticles [21].

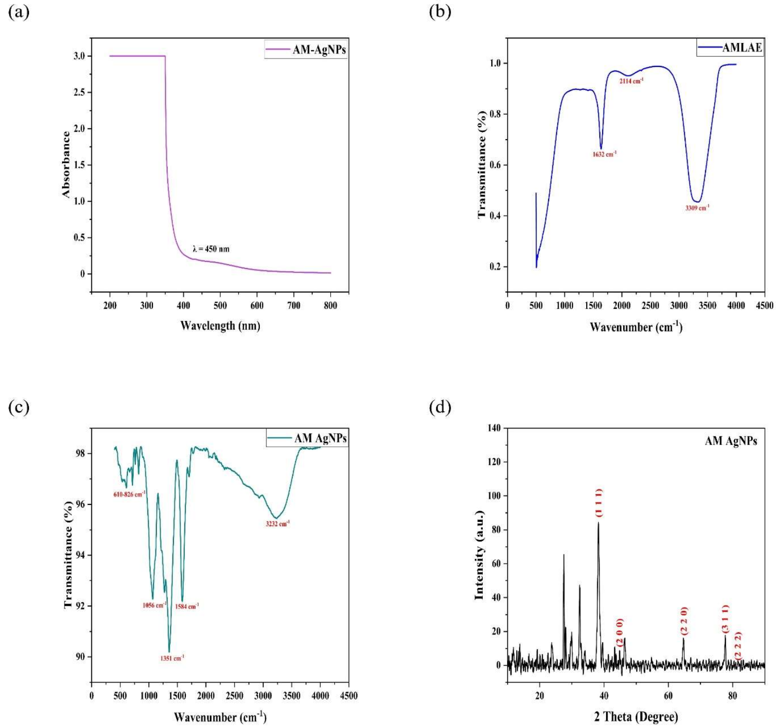

Figure 1: LSPR, Surface functionalization and Phase analysis of AM-AgNPs (a) UV-Vis absorbance spectrum (b) AMLAE FTIR spectrum (c) AM-AgNPs FTIR spectrum and (d) X-ray diffractogram of AM-AgNPs.

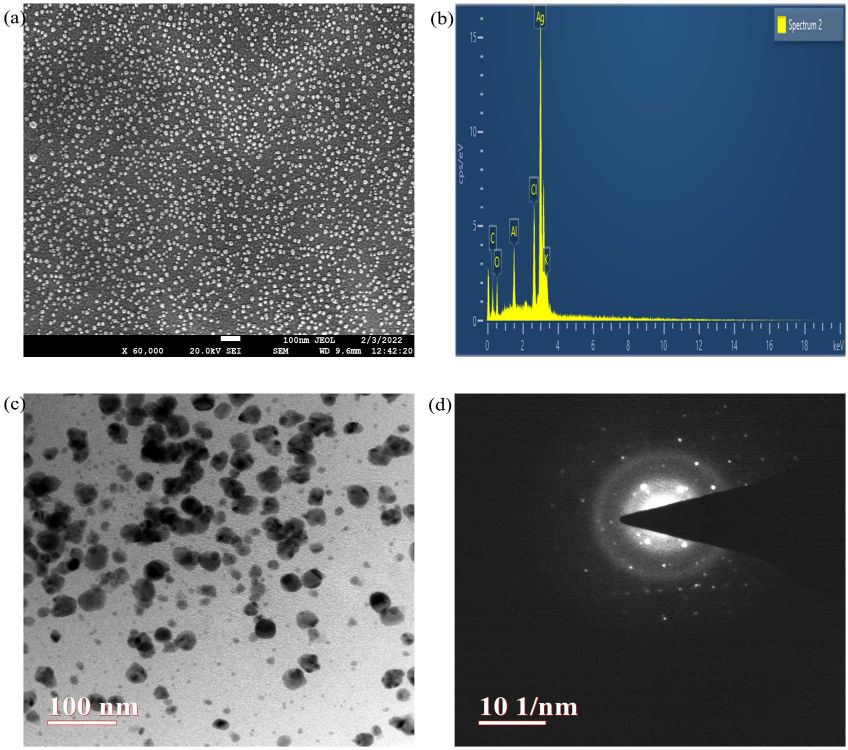

Figure 2: Electron Microscopy analysis of AM-AgNPs (a) FESEM Micrograph (b)EDAX spectrum (c) HRTEM Micrograph and (d) SAED pattern

3.3. Antimicrobial Activity:

The antimicrobial efficacy of AM-AgNPs was determined in terms of MIC using a dilution micro broth assay with concentrations ranging from 1000 to 3.9 μg mL^{-1} on 6 microbial species. However, AM-AgNPs had the lowest MIC range against G-ve bacteria, specifically *V. parahaemolyticus* (15.62 μg mL^{-1}) and *V. harveyi* (62.5 μg mL^{-1}). On the other hand, they had higher MIC ranges against G+ve bacteria and fungi (Fig. 3(d)). Inhibition of microbial growth at high concentrations of AgNPs limits their applications in real time and may also cause toxicity toward life and the environment [22]. Green-synthesized AgNPs are effective in antimicrobial properties due to the synergism of plant phytochemicals and Ag. But challenges associated with green synthesis are phytochemicals and their quantity differing among geographical regions, extraction procedures, thermolabile phytocompounds, fungal contamination, etc. Purifying bioactive compounds from plants and using them as reducing agents could overcome these challenges and produce nanoparticles with homogeneous size and shape [23]. Recent studies on synthesis of AgNPs using leaf aqueous extracts of *Mirabilis jalapa* [24] and *Euphorbia hitra* [17] shown efficient antimicrobial activity on *V. parahaemolyticus* and *V. harveyi*. Therefore, improving the surface properties of AgNPs could result in more efficient antimicrobial properties to combat the increased incidences of AMR.

3.4. Photocatalytic Degradation of MB:

Photocatalytic degradation of 50 ppm aqueous methylene blue (MB) solution by AM-AgNPs was assessed under visible light irradiation for 60 minutes with every 10-minute interval. At a concentration 100 μg mL^{-1} of AM-AgNPs, 99.24% of MB was degraded at 60 minutes. The degradation (%) of MB against time was represented in Fig 4(a).

3.5. Vero Cell Cytotoxicity:

The synthesis of AgNPs using green routes and green reducing agents necessitates determining their toxicity towards life and the environment. Apart from their antimicrobial activity, the present study aims to evaluate the cytotoxicity of AM-AgNPs on Vero cell lines, healthy cell lines derived from *Cercopithecus aethiops* kidney epithelial cells. Upon exposure to the various concentrations of AM-AgNPs (0–200 μg mL^{-1}), the concentration-dependent decrease in Vero cell viability was observed (0–64.54%), which was observed using the MTT assay (Fig 4 (b) & (c)). The calculated IC_{50} value of AM-AgNPs was 253.73 μg mL^{-1}; this indicates that the addition of IC_{50} concentration of AM-AgNPs is able to kill 50% of healthy cells. Previous studies reported that selenium NPs synthesized using extract of *Allium sativum* exhibited an IC_{50} concentration of 31.8 μg mL^{-1} [25], whereas AgNPs synthesized using *Catharanthus roseus* exhibited 589 μg mL^{-1} of IC_{50} concentration [26]. A higher IC_{50} concentration is inversely proportional to the toxicity of healthy cell lines. Several hypothetical mechanisms were proposed on cytotoxicity patterns of AgNPs, and the most common one is generating the oxidative stress ultimately leading to the disruption of cell organelles and cell membranes [27], [28].

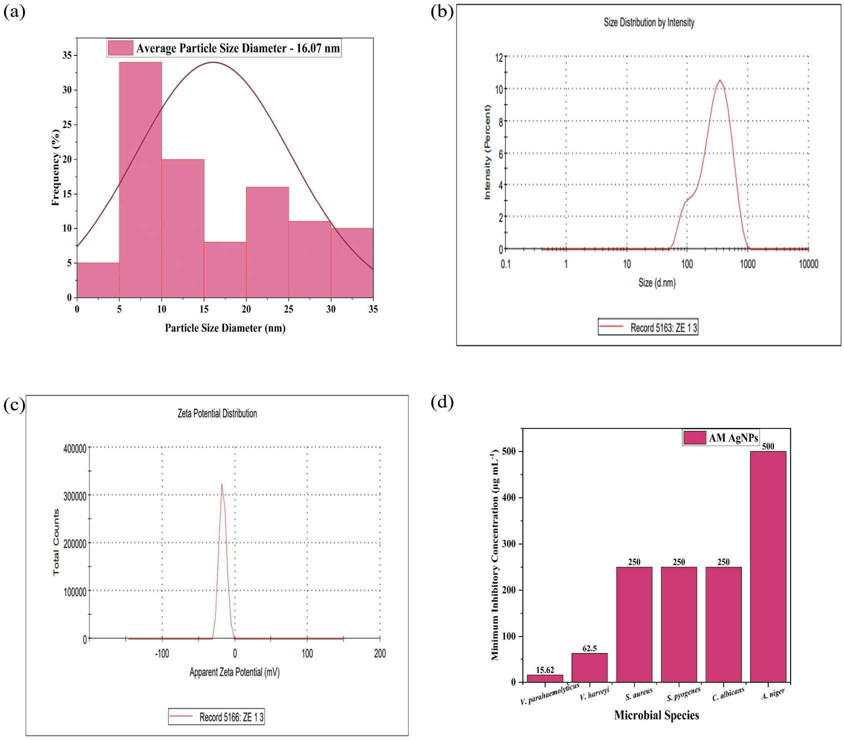

Figure 3: DLS and Antimicrobial activity of AM-AgNPs (a) Particle size diameter histogram (b) Hydrodynamic size (c) Zeta potential and (d) Antimicrobial activity.

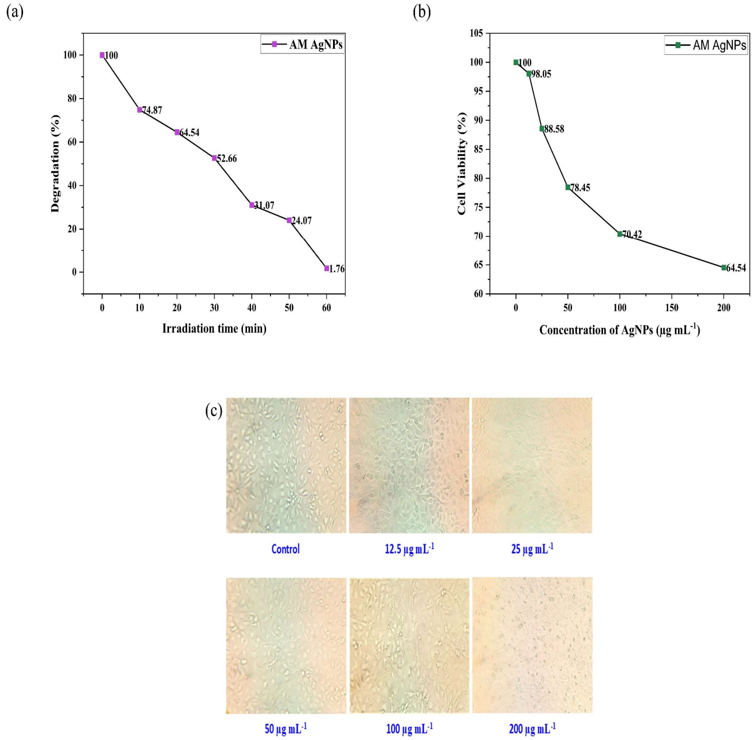

Figure 4: Photocatalytic and healthy cell line cytotoxicity of AM-AgNPs (a) Photocatalytic degradation of methylene blue (b) Concentration dependent cell viability and (c) Morphological alterations of Vero cell lines treated with various concentrations of AM-AgNPs.

Previous studies reported the synthesis of AgNPs using various parts of Bael and the reducing agent prepared using various methods is reported in table 1.

Table 1: Comparative analysis of size, shape and activities of AgNPs synthesized using Bael.

S.No	Part of the plant (AM)	Phyto-chemical extraction method	AgNPs size	AgNPs shape	Activity/Application	Reference
1	Leaves	Decoction (Distilled Water)	30-50 nm	Spherical	Antimicrobial, Antioxidant, Anticancer and Photocatalytic degradation of basic fuchsin dye	[10]
2	Fruit	Agitation/Maceration (Methanol)	10-200 nm	Spherical	Antimicrobial	[14]
3	Leaves	Decoction (Distilled Water)	60 nm	Spherical	No reported application/activity	[11]
4	Fruit	Decoction (Distilled Water)	_	_	Antibiofilm assay	[15]
5	Leaves	Decoction (Distilled Water)	5-30 nm	Spherical and irregular	Antibacterial, Antilarvicidal, Photocatalysis and Cytotoxicity activities.	[12]
6	Leaves	Decoction (Distilled Water)	_	_	Antibacterial activity	[13]
7	Bark	Decoction (Distilled Water)	20 nm	Spherical	DNA cleavage, DNA binding, antioxidant and antibacterial activities	[16]

4. Conclusion:

The green approach for the synthesis of AgNPs using AMLAE was successfully achieved, with AMLAE functioning as a reducing and stabilizing agent. The structural and functional properties of AM-AgNPs were confirmed through various analytical techniques, including UV-Vis spectroscopy, FTIR, XRD, HRTEM, and DLS. The nanoparticles exhibited spherical morphology with an average crystallite size of 14.07 nm and a hydrodynamic size of 237.5 nm. The antimicrobial activity showed effective inhibition of pathogens, with a minimum inhibitory concentration of 15.62 µg mL^{-1}. for *Vibrio parahaemolyticus*. Photocatalytic degradation experiments revealed a 99.24% efficiency in degrading methylene blue under visible light within 60 minutes. Cytotoxicity studies on Vero cell lines indicated an IC_{50} value of 253.73 µg mL^{-1}, demonstrating low toxicity within the tested concentration range. Future work should focus on understanding the detailed molecular mechanisms involved in the AMLAE-mediated synthesis process and exploring the impact of varying synthesis parameters on nanoparticle properties. Expanding applications to real-world scenarios such as wastewater treatment, antimicrobial coatings, and biomedicine is necessary. Comprehensive in vivo studies on biocompatibility and therapeutic efficacy will further establish the potential of these nanoparticles. Using purified phytochemicals from *Aegle marmelos* could enhance the consistency and functionality of nanoparticles, supporting their application in diverse industrial and medical fields.

5. Acknowledgments. Not applicable

6. Disclosure of Interests. The authors declare no competing interests.

7. References

1. S. Bayda, M. Adeel, T. Tuccinardi, M. Cordani, and F. Rizzolio, “Molecules-25-00112-V2.Pdf,” *Molecules*, vol. 25, no. Figure 1, pp. 1–15, 2020.
2. Praveena, V. Durga, G. Tejaswini, and M. Padmaja. "An innovative adsorption of thiocyanate ions in aqueous solutions by exploiting eco-ZnO nanoparticles." *Inorganic Chemistry Communications* (2023): 111708.
3. Y. Guo *et al.*, “Mechanisms of chemotherapeutic resistance and the application of targeted nanoparticles for enhanced chemotherapy in colorectal cancer,” 2022, *BioMed Central*. doi: 10.1186/s12951-022-01586-4.
4. Padmaja, M., Shyamala, P., Praveena, V. D., & Tejaswini, G. (2024). Green synthesized Fe3O4@ CD nanocomposites using Acacia caesia leaves: In vitro biological properties and cytotoxicity assessment. *Next Nanotechnology*, *6*, 100093.
5. K. Chand *et al.*, “Green synthesis, characterization and photocatalytic application of silver nanoparticles synthesized by various plant extracts,” *Arab. J. Chem.*, vol. 13, no. 11, pp. 8248–8261, 2020, doi: 10.1016/j.arabjc.2020.01.009.
6. S. Ahmad *et al.*, “Green nanotechnology : a review on green synthesis of silver nanoparticles — an ecofriendly approach,” 2019.
7. Praveena, V. Durga, and K. Vijaya Kumar. "Synthesis and characterization of chitosan based silver nano composite system for antibacterial applications." *International*

Conference on Advanced Nanomaterials & Emerging Engineering Technologies. IEEE, 2013.

8. M. T. Rahman, M. A. Halim, N. H. M. R. Mozumder, T. A. Ove, and A. A. Khatun, “Phytochemicals and antioxidant properties of bael (Aegle marmelos L.) pulp powder and its products,” *J. Agric. Food Res.*, vol. 15, p. 100971, 2024, doi: https://doi.org/10.1016/j.jafr.2024.100971.
9. C. K. Pathirana, T. Madhujith, and J. Eeswara, “Bael (Aegle marmelos L. Corrêa), a Medicinal Tree with Immense Economic Potentials,” *Adv. Agric.*, vol. 2020, no. 1, p. 8814018, Jan. 2020, doi: https://doi.org/10.1155/2020/8814018.
10. P. Rama, P. Mariselvi, R. Sundaram, and K. Muthu, “Eco-friendly green synthesis of silver nanoparticles from Aegle marmelos leaf extract and their antimicrobial, antioxidant, anticancer and photocatalytic degradation activity,” *Heliyon*, vol. 9, no. 6, p. e16277, 2023, doi: https://doi.org/10.1016/j.heliyon.2023.e16277.
11. K. Jagajjanani Rao and S. Paria, “Green synthesis of silver nanoparticles from aqueous Aegle marmelos leaf extract,” *Mater. Res. Bull.*, vol. 48, no. 2, pp. 628–634, 2013, doi: 10.1016/j.materresbull.2012.11.035.
12. G. Sampath *et al.*, “Eco-friendly biosynthesis metallic silver nanoparticles using Aegle marmelos (Indian bael) and its clinical and environmental applications,” *Appl. Nanosci.*, vol. 13, no. 1, pp. 663–674, 2023, doi: 10.1007/s13204-021-01883-8.
13. J. S. G. Christopher, B. Saswati, and P. S. Ezilrani, “Optimization of parameters for biosynthesis of silver nanoparticles using leaf extract of Aegle marmelos,” *Brazilian Arch. Biol. Technol.*, vol. 58, no. 5, pp. 702–710, 2015, doi: 10.1590/S1516-89132015050106.
14. M. Devi, S. Devi, V. Sharma, N. Rana, R. K. Bhatia, and A. K. Bhatt, “Green synthesis of silver nanoparticles using methanolic fruit extract of Aegle marmelos and their antimicrobial potential against human bacterial pathogens,” *J. Tradit. Complement. Med.*, vol. 10, no. 2, pp. 158–165, 2020, doi: 10.1016/j.jtcme.2019.04.007.
15. N. D. A. Krupa and V. Raghavan, “Biosynthesis of silver nanoparticles using aegle marmelos (Bael) fruit extract and its application to prevent adhesion of bacteria: A strategy to control microfouling,” *Bioinorg. Chem. Appl.*, vol. 2014, 2014, doi: 10.1155/2014/949538.
16. A. De, P. Jain, A. K. Manna, V. Srivastava, and R. Das, “An eco-benign synthesis of silver nanoparticles using Aegle marmelos L. bark extract and evaluation of their DNA cleavage, DNA binding, antioxidant and antibacterial activity,” *Inorg. Nano-Metal Chem.*, vol. 54, no. 1, pp. 6–17, Jan. 2024, doi: 10.1080/24701556.2021.2007129.
17. A. Marukurti *et al.*, “Evaluation of anti-vibriocidal, antioxidant properties and cytotoxicity of bio fabricated/green synthesized silver nanoparticles using Euphorbia hitra L. leaf extract,” *Next Mater.*, vol. 7, p. 100355, 2025, doi: https://doi.org/10.1016/j.nxmate.2024.100355.
18. V. N. Pangi, A. Marukurti, A. M. Reddy, and S. R. Medapalli, “Synthesis of Biogenic Silver Nanoparticles (bAgNPs) Using Leaf Extract of Mirabilis jalapa and Evaluation of Anti-vibriocidal, Anti-oxidant properties and Cytotoxicity,” *Bionanoscience*, vol. 13, no. 2, pp. 376–392, 2023, doi: 10.1007/s12668-023-01060-x.
19. A. Wirwis and Z. Sadowski, “Green Synthesis of Silver Nanoparticles: Optimizing Green Tea Leaf Extraction for Enhanced Physicochemical Properties,” *ACS Omega*,

vol. 8, no. 33, pp. 30532–30549, 2023, doi: 10.1021/acsomega.3c03775.
20. S. N. A. Mat Yusuf, C. N. A. Che Mood, N. H. Ahmad, D. Sandai, C. K. Lee, and V. Lim, “Optimization of biogenic synthesis of silver nanoparticles from flavonoid-rich Clinacanthus nutans leaf and stem aqueous extracts,” *R. Soc. Open Sci.*, vol. 7, no. 7, 2020, doi: 10.1098/rsos.200065.
21. A. P. Ramos, “4 - Dynamic Light Scattering Applied to Nanoparticle Characterization,” in *Nanocharacterization Techniques*, A. L. Da Róz, M. Ferreira, F. de Lima Leite, and O. N. Oliveira, Eds., in Micro and Nano Technologies. , William Andrew Publishing, 2017, pp. 99–110. doi: https://doi.org/10.1016/B978-0-323-49778-7.00004-7.
22. M. S. Akhter *et al.*, “A systematic review on green synthesis of silver nanoparticles using plants extract and their bio-medical applications,” *Heliyon*, vol. 10, no. 11, p. e29766, 2024, doi: 10.1016/j.heliyon.2024.e29766.
23. J. E. Castañeda-Aude, J. R. Morones-Ramírez, D. A. De Haro-Del Río, A. León-Buitimea, E. D. Barriga-Castro, and C. E. Escárcega-González, “Ultra-Small Silver Nanoparticles: A Sustainable Green Synthesis Approach for Antibacterial Activity,” *Antibiotics*, vol. 12, no. 3, 2023, doi: 10.3390/antibiotics12030574.
24. V. N. Pangi, A. Marukurti, A. M. Reddy, and S. R. Medapalli, “Synthesis of Biogenic Silver Nanoparticles (bAgNPs) Using Leaf Extract of Mirabilis jalapa and Evaluation of Anti-vibriocidal, Anti-oxidant properties and Cytotoxicity,” *Bionanoscience*, no. 0123456789, 2023, doi: 10.1007/s12668-023-01060-x.
25. K. Anu, G. Singaravelu, K. Murugan, and G. Benelli, “Green-Synthesis of Selenium Nanoparticles Using Garlic Cloves (Allium sativum): Biophysical Characterization and Cytotoxicity on Vero Cells,” *J. Clust. Sci.*, vol. 28, no. 1, pp. 551–563, 2017, doi: 10.1007/s10876-016-1123-7.
26. K. Jamil *et al.*, “Biogenic Synthesis of Silver Nanoparticles Using Catharanthus roseus and Its Cytotoxicity Effect on Vero Cell Lines,” *Molecules*, vol. 27, no. 19, pp. 1–18, 2022, doi: 10.3390/molecules27196191.
27. V. A. Online, “Environmental Science : Processes & Impacts,” pp. 78–92, 2013, doi: 10.1039/c2em30595j.
28. Z. Xiu, Q. Zhang, H. L. Puppala, V. L. Colvin, and P. J. J. Alvarez, “Negligible Particle-Speci fi c Antibacterial Activity of Silver Nanoparticles,” 2012.